Toughening and Reinforcement of Rigid PVC with Silicone Rubber/Nano-CaCO$_3$ Shell-Core Structured Fillers

Ling Yang,[1] Yuan Hu,[1] Hong Guo,[1] Lei Song,[1,2] Zuyao Chen,[2] Weicheng Fan[1]

[1]State Key Laboratory of Fire Science, University of Science and Technology of China, 230026 Anhui, People's Republic of China
[2]Department of Chemistry, University of Science and Technology of China, 230026 Anhui, People's Republic of China

ABSTRACT: To improve the mechanical properties and structure of poly(vinyl chloride) (PVC)/nano-CaCO$_3$ nanocomposite, a core (nano-CaCO$_3$)/shell (SR) structured filler (40–60 nm) was successfully prepared by refluxing methyl vinyl silicone rubber (SR) and nano-CaCO$_3$ particles (coupling agent KH550, KH560, or NDZ-101 as interfacial modifier) in toluene with vigorous stirring, according to an encapsulation model. It is effective in rigid PVC composite's toughness and reinforcement. The interfacial modifier's structure and interaction of nano-composites of PVC/SR/nano-CaCO$_3$ were studied. The results indicate that KH560 has the optimal interfacial modificatory effect. The environmental scanning electron microscope (ESEM) study testified that PVC/SR/nano-CaCO$_3$ nanocomposites had a typical rubber–plastics-toughening mechanism. © 2006 Wiley Periodicals, Inc. J Appl Polym Sci 102: 2560–2567, 2006

Key words: poly(vinyl chloride); nanocomposites; core-shell polymers; morphology; mechanical properties

INTRODUCTION

Polymer blends are of significant importance because blending could provide a means for improving mechanical properties as well as processability. On the other hand, incorporation of rubbery polymers lowers the tensile strength,[1] resistance to heat, and processing behavior of plastics,[2] and so it is highly important for theory and practice to look for better methods of plastics toughening.

In the study of the toughening of common plastics, poly(vinyl chloride) (PVC) toughening has attracted great interest owing to its low price and good resistance to aging and corrosion. In the recent decade, scientists have already studied elastomer as filler in PVC matrix to improve the processing properties of PVC and achieve rubber–plastics-toughening of rigid PVC materials.[3–6] But one of the most promising means in preparing inorganic–organic nanocomposite via melt blending, such as PVC–clay nanocomposites,[7–9] were reported successively. Other nanoparticles such as nanometric CaCO$_3$, SiO$_2$, TiO$_2$, and ZnO particles have been used to prepare nanocomposites.[10–13] And nano-CaCO3 has been one of the most commonly used inorganic fillers for PVC.[14–16] Wu et al. studied the mechanical properties, morphology, and rheology of the system chlorinated polyethylene (CPE)/nano-CaCO$_3$ master batch as reinforcement filler in PVC; CPE as an interfacial modifier were studied.[15] Although CPE/nano-CaCO$_3$ master batch has a high toughening effect for PVC, using CPE increases the content of halogen in material and limits material's using area.

The goal of the present study was to investigate the probability of toughening of PVC filled with nano-CaCO$_3$ particles. To eliminate incompatibility between inorganic–organic interfaces, silicone rubber (SR) was used as an interfacial modifier. For this purpose, a kind of master batch of SR/nano-CaCO$_3$ particles was prepared via refluxing nano-CaCO$_3$ in toluene solution of SR. The master batch was employed as filler to prepare nanocomposites with PVC via a melt mixing; the mechanical properties and morphology were investigated. The correlation between the mechanical properties and morphology of nanocomposites was established. The toughening mechanisms were also proposed.

TABLE I
Organo-Functional Coupling Agent Structure

KH550	$N_2H-CH_2CH_2CH_2-Si(OC_2H_5)$
KH560	$Cl-CH_2CH_2CH_2-Si(OC_2H_5)$
NDZ-201	$CH_3-CH-O-Ti-(O-P-O-P-O-C_8H_{17})_2$

EXPERIMENTAL

Materials

A suspension PVC (S1000, MW: 62,500) employed in this study was purchased from Qilu Petrochemical, Shandong Province, China. Methyl vinyl silicone rubber (MVMQ, 110-2), with a vinyl content of 0.17%, was commercially obtained from Dongjue Fine Chemicals (Nanjing). Nano-CaCO$_3$ fillers with an average particle diameter of 40 nm were supplied by Nano-Tech Science and Technology Company, Beijing, China. The filler was surface treated with coupling agent (Table I) of silane coupling agent KH550 and KH560, titanate coupling agent NDZ-101 by the manufacturer from Nanjing ShuGuang Chemical General Company. The treatment method is described as follows: the required volume of the coupling agent was diluted with an equal amount of toluene, and a 1:1 solution was formed. The diluted solution was slowly sprayed, for 10-min periods, on the nano-CaCO$_3$ filler contained in a rotating mixer of the Sigma type. The rotation direction of the mixer was changed every 5 min to ensure distribution of the coupling agents in the nano-CaCO$_3$ filler. The additives, such as a lead complex thermal stabilizer, calcium stearate, and external wax, were provided by Haolong Chemical, Tianjin, China.

SAMPLE PREPARATION

Preparation of SR/nano-CaCO$_3$ master batch

A given weight of MVMQ (4 g) was dispersed in 180 mL toluene and stirred at 90°C till MVMQ swelled in toluene completely; nano-CaCO$_3$ (15 g) was scattered into a small amount of toluene before dispersing in MVMQ. The mixture was heated and refluxed for 2 h at 90°C with vigorous stirring, after that the product was dried at 75°C for 16 h, then the MVMQ coating nano-CaCO$_3$ particles were homogenized by grinding in an agate mortar and ready for using in PVC formulations.

Preparation of PVC nanocomposites

The rigid PVC formulations were mixed on the two-roll mill at 160–165°C for 10 min, then the resulting mixtures were cooled to room temperature for upper testing. Table II shows the PVC formulations.

ANALYSES AND CHARACTERIZATION

The morphology of MVMQ coating nano-CaCO$_3$ particles was evaluated using bright field transmission electron microscopy (TEM). All of the particles of nano-CaCO$_3$ and SR/nano-CaCO$_3$ master batch were dispersed in ethanol in an ultrasonic bath for 10 min. TEM images were obtained on a JEOL JEM-100SX microscope with an acceleration voltage of 80 kV.

The morphology of PVC sample's tensile fractured surface tore in tensile testing and fractured surface obtained in Notched Izod impact test were studied by environmental scanning electron microscope (ESEM) examination: all the tensile fractured surfaces were coated with gold–palladium film. The center of the fractured surface for each sample was examined on PHILIPS XL 30 ESEM-TMP.

The tensile tests were carried out using a Universal Testing Machine DCS-5000 (Shimadzu, Japan) at a head speed of 200 mm/min according to ASTM D-638. All measurements were repeated five times and the values averaged.

The shore A hardness was obtained from LX-A Rubber–Plastics Shore A Sclerometer (Mingzhu Instruments, Jiangdu) according to GB T 531 92.

Notched Izod impact strength was measured with a SUMITOMO impact tester according to the standard of ASTM D256 at room temperature. The thickness of the Izod impact specimens was 1/8 in., and the impact energy was 4 J.

The Fourier transform infrared (FTIR) spectra were recorded using a Nicolet MAGNA-IR 750 spectrometer using a thin film.

TABLE II
Summary of Rigid PVC Compounds

Sample code	PVC (g)	DOTP (g)	TBLS (g)	St (g)	BPA (g)	Packed nano-CaCO$_3$ (g)
EPVC0	100	40	4	0	0.5	None
EPVC1	100	40	4	0.3	0.5	15 (melt blending directly, without modification)
EPVC2	100	40	4	0.3	0.5	15 (coated, without modification)
EPVC3	100	40	4	0.3	0.5	15 (coated, modified by KH550 coupling agent)
EPVC4	100	40	4	0.3	0.5	15 (coated, modified by KH560 coupling agent)
EPVC5	100	40	4	0.3	0.5	15 (coated, modified by NDZ-101 coupling agent)

St, Styrene; BPA, Bisphenol-A.

A differential scanning calorimeter (PerkinElmer Diamond DSC) was used to examine the thermal properties of the rigid PVC/SR/nano-CaCO$_3$ nanocomposites at a heating rate of 20°C/min under a nitrogen flow. The sample was two-stage-heated. First, the sample was heated from 30 to 80°C and then cooled to room temperature to release the internal stress of the sample. Second, the sample was reheated from 35 to 120°C at a heating rate of 20°C/min. The T_g of the rigid PVC/SR/nano-CaCO$_3$ nanocomposite was recorded and analyzed.

RESULTS AND DISCUSSIONS

Figure 1(a) testifies that nano-CaCO$_3$ particles are easy to aggregate and result in asymmetric sizes from 40 to 250 nm. But Figure 1(b–e) shows that the coating of SR prevents nano-CaCO$_3$ particles' aggregation, and so the particles of master batch are symmetrical and the sizes are about 20–60 nm; the SR shell prevents the aggregation of nano-CaCO$_3$ particles effectively. A reason for this may be the low surface energy of this kind of SR and its high molar mass, which causes it to cover other particles easily and prevents nano-CaCO$_3$ particles' aggregation.[17]

Mechanical properties

Impact strength is one of the most important mechanical properties of plastic–rubber blends since it determines the utility of these materials. It is generally believed that the interfacial adhesion between the dis-
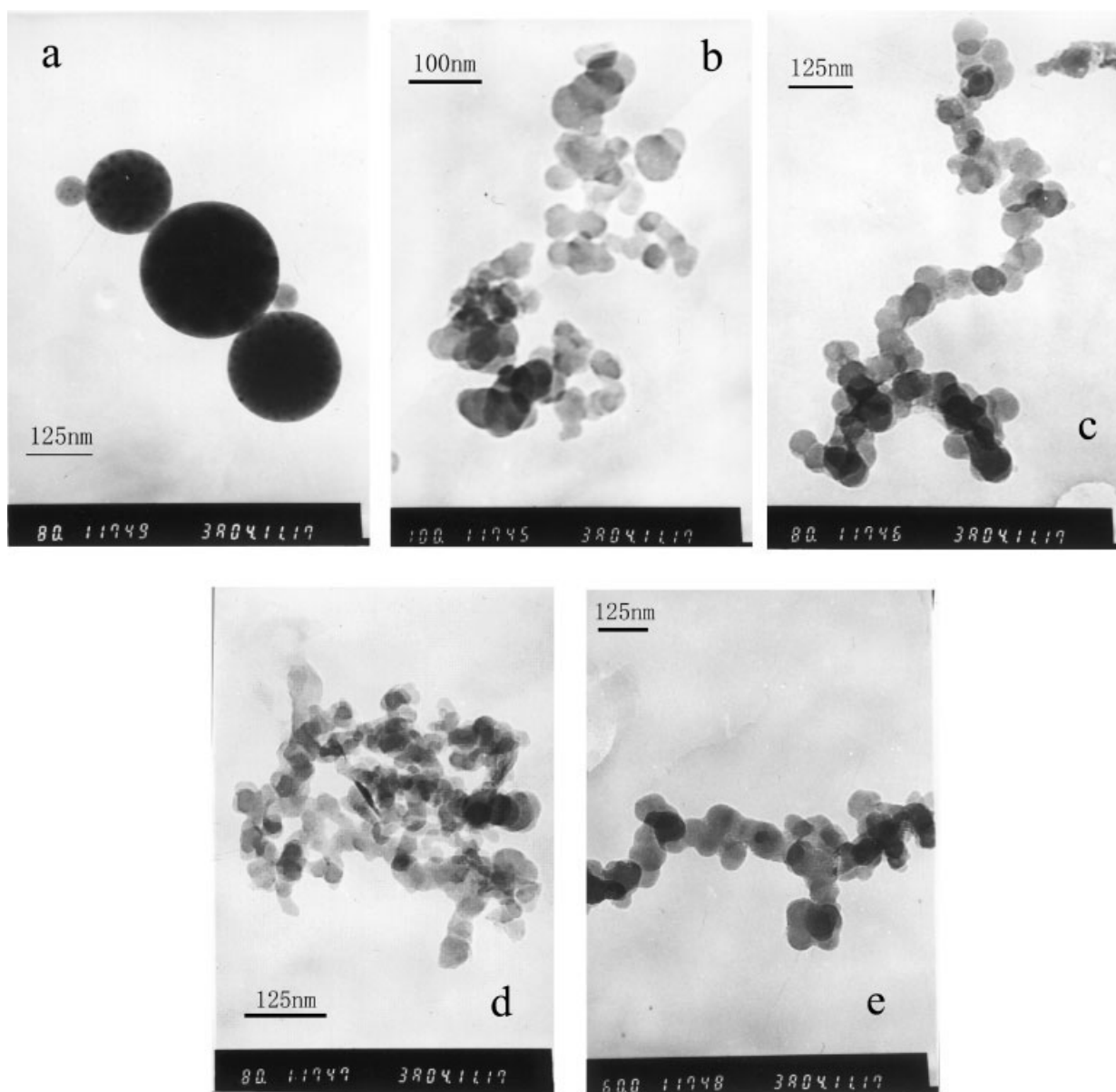

Figure 1 TEM micrographs of (a) nano-CaCO$_3$ particles and (b)–(e) SR/nano-CaCO$_3$ master batch.
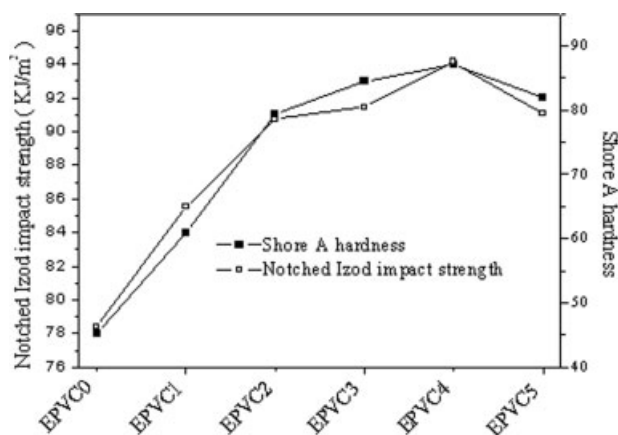
Figure 2 Notched Izod impact strength and Shore A hardness of PVC/nano-CaCO₃ nanocomposites versus different coupling agent.

persed rubber particles and the matrix plays an important role in the toughening of polymers. Figure 2 presents the notched Izod impact strength and Shore A hardness of PVC/nano-CaCO₃ nanocomposites using different coupling agent, which indicated that the nano-CaCO₃ particles had a remarkable toughening effect on PVC. The impact strength of pure PVC (sample EPVC0) was 46.2 kJ/m^2, and it increased slightly to 64.9 kJ/m^2 for the PVC/SR/nano-CaCO₃ melt blending directly (sample EPVC1), but increased acutely for PVC/master batch nanocomposites; the impact strength of EPVC4 is high up to 87.5 kJ/m^2. Shore A hardness are all increased compared with that of EPVC0. It is obvious that the toughening efficiency of SR/nano-CaCO₃ master batch on PVC is much higher than that of normal nano-CaCO₃ fillers.

The strength and elongation at break of PVC/nano-CaCO₃ nanocomposites and PVC/SR/nano-CaCO₃ nanocomposites are presented in Figure 3. The PVC/SR/nano-CaCO₃ nanocomposites melt blending directly (sample EPVC1) exhibited a distinctly higher tensile strength than that of pure PVC, which revealed that not only the nano-CaCO₃ particles gave a strength enhancement on the PVC matrix, but also SR had a lubricant effect which made nano-CaCO₃ particle have a good dispersion. However, a further increase in the tensile strength and elongation at break of PVC sample using SR/nano-CaCO₃ master batch, especially sample EPVC4, nano-CaCO₃ particles were modified by KH560 coupling agent, had the best tensile strength (24.9 MPa) and the longest elongation at break (390.98%).

From the mechanical properties, it can be concluded that the dispersion effect of the shell-core structured SR/nano-CaCO₃ master batch are better than that of nano-CaCO₃, and SR/nano-CaCO₃ master batch have better reinforcing effect on PVC matrix.

ESEM morphological analysis

For further study of the mechanisms of reinforcement effect of SR/nano-CaCO₃ for PVC, electromicroscopy was employed. Figures 4 and 5 give the morphology of PVC samples' divulsive surface torn in tensile testing at different amplifier. From the comparison of Figure 4(b–f) with Figure 4(a) and Figure 1, it can be obtained that the usage of SR (including melt blending directly), although does not prevent completely the particles from aggregation, can effectively reduce nano-CaCO₃ particles' size to improve particles' dispersion in PVC matrix. There are many "filaments" in tensile fractured surface except sample EPVC0 [Fig. 4(a)]. But there are regular tropism structure be similar to fascicules in EPVC4 [Fig. 4(e)].

Figure 5 shows the morphology at high amplifier. Figure 5(a) is the morphology of sample EPVC0's tensile fractured surface, it is obvious that there is substantial debonding of two phases before yielding in the composites, and the surface of CaCO₃ particles are perfectly clean. It can be concluded that there is almost no adhesion between CaCO₃ particles and PVC matrix, so EPVC0 has the worst mechanical properties. On the other hand, Figure 5(b–f) testify that PVC compounds reinforced by SR/nano-CaCO₃ master batch have different morphology. Apart from some agglomerated particles, a relatively good dispersion is clearly seen. And there are many "filaments," shown in Figure 5(b–d) and Figure 5(f), the "filaments" are mainly occurring between SR/nano-CaCO₃ particles, this phenomenon shows that the "filaments" are the coating of SR formed during the tensile process. In Figure 5(e), because of better miscibility of PVC and SR/nano-CaCO₃ master batch for effect of KH560 coupling agent, the "filaments" consists not only of SR but also part of PVC matrix, so the "filaments" is tangled up on the surface of the PVC/SR/nano-CaCO₃ nanocomposites. But there is a kind
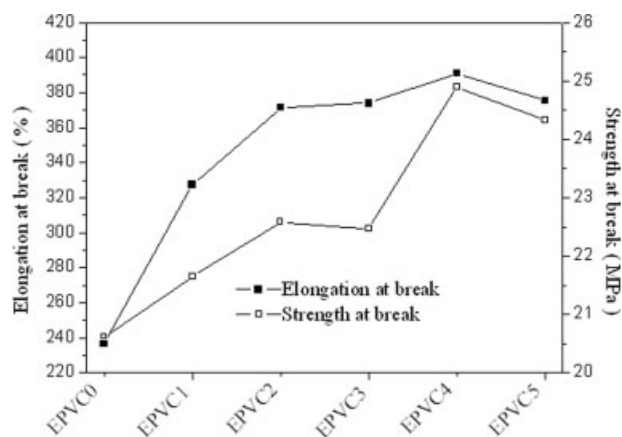

Figure 3 Strength and elongation at break of PVC/nano-CaCO₃ nanocomposites versus different coupling agent.
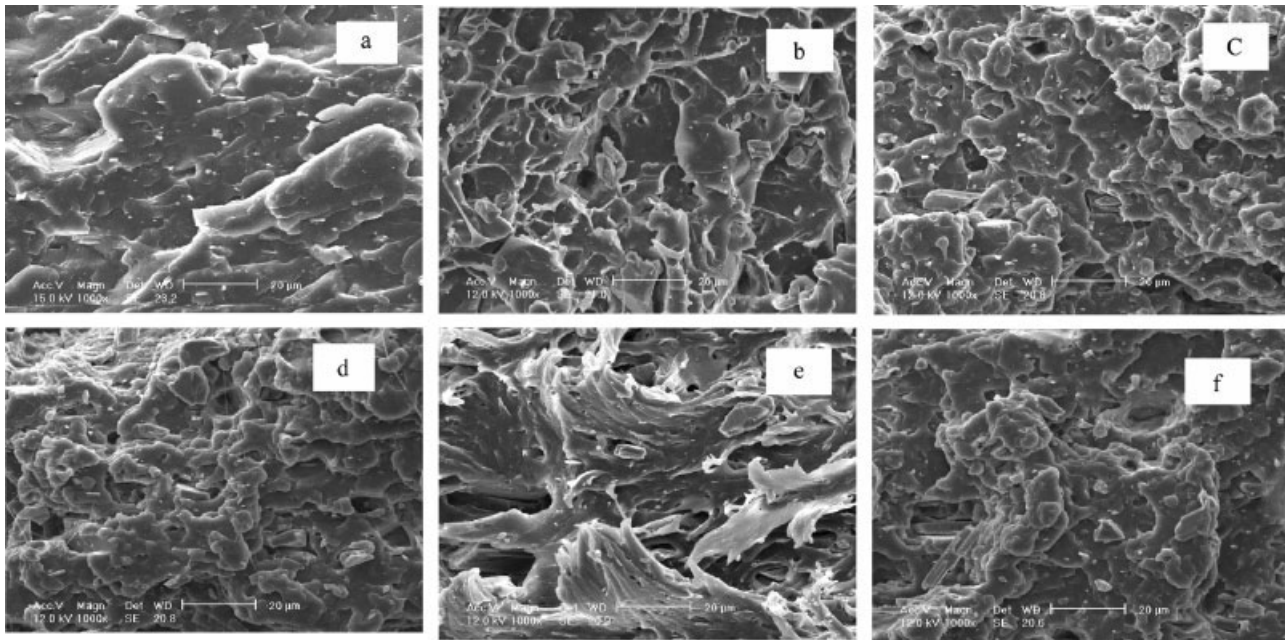
Figure 4 ESEM micrographs of tensile-fractured surfaces of PVC nanocomposites (×1000): (a) EPVC0; (b) EPVC1; (c) EPVC2; (d) EPVC3; (e) EPVC4; (f) EPVC5.

of structure such as region marked C. Figure 6 gives the morphology of region "C". It is obvious that there is an excellent adhesion between master batch particles and PVC matrix; the two phase structure disappears and many regular and strong tropistic fasciculus slice-layered structures are formed on the tensile-fractured surfaces which apparently bond the two phases together (region marked A and B).

The scheme for interactions of the PVC/nano-CaCO$_3$ composite and PVC/SR/nano-CaCO$_3$ are

shown in Figure 11. Owing to the incorporation of coupling agent into the composites, the strong interaction between the filler and polymer transformed structurally the composite into an interpenetrating polymer network, during the tensile process regular tropism fasciculi are formed and arranged orderly to form slice-layered structure.

The toughening of PVC by microsized CaCO$_3$ particles could be explained by the crack front bowing mechanism.[18] However, the size of nano-CaCO$_3$ par-

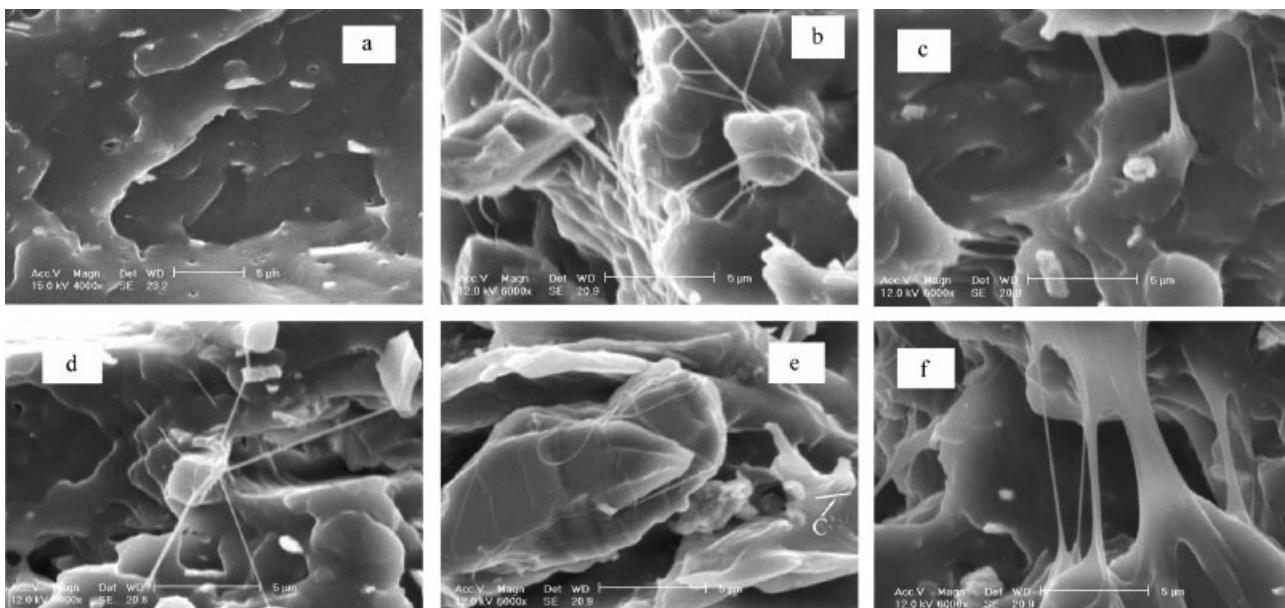**Figure 5** ESEM micrographs of tensile-fractured surfaces of PVC nanocomposites (×6000): (a) EPVC0; (b) EPVC1; (c) EPVC2; (d) EPVC3; (e) EPVC4; (f) EPVC5.
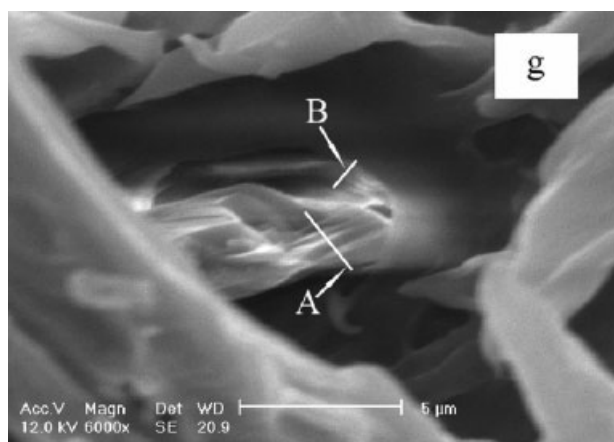
Figure 6 ESEM image of the region signed as ''C'' in Figure 5e (×6000).

ticles used in this study is from several 10 nm to several 100 nm (because of serious aggregation), and particle of SR/nano-CaCO$_3$ is 40–60 nm, the applicability of the bowing mechanism is questionable, because such small-sized rigid particles may not be able to resist the propagation of the crack. Obviously, the toughening effect of SR/nano-CaCO$_3$ master batch on PVC could be contributed to a new mechanism. Such a high toughening effect for PVC/elastomer/nano-CaCO$_3$ nanocomposites was attributable to a typical rubber–plastics-toughening mechanism.[4,6,15]

To evaluate the toughening mechanism, we studied the fractured surfaces in Notched Izod impact test. Figure 7 reveals the ESEM photographs of the fractured surfaces of PVC composites. Similar to the tensile behavior, pristine PVC exhibits brittle failure; but the nanocomposites contained SR show ductile

characteristics. Several long shearing bands are parallelized to each other and few cavitations emerge on the fracture surface of sample EPVC4 in which SR/nano-CaCO$_3$ master batch were modified with KH560 [Fig. 7(e)], indicating that the PVC/SR/nano-CaCO$_3$ modified with KH560 blend fractures in a ductile mode. Meanwhile, the shearing bands become quite short and less orientational, and a high degree of cavitation is found on the fracture surface of the sample EPVC3 and EPVC5 in which SR/nano-CaCO$_3$ master batch were modified with KH550 and NDZ-101, respectively, [Fig. 7(d and f)]. And there are only some ''filaments'' [Fig. 7(b and c)], that represent sample EPVC1 and EPVC2, respectively, but in Figure 7(b) there are more cavitations than that in Figure 7(c). All these phenomena suggest that the rigid PVC samples with SR have better compatibility, and the coupling agents lead to inseparable interaction between PVC matrix and SR/nano-CaCO$_3$ master batch. Along with the increasing interphase compatibility of the PVC matrix and SR/nano-CaCO$_3$, the PVC/SR/nano-CaCO$_3$ nanocomposites have tighter and tighter microstructures with less cavitation, so these PVC nanocomposites not only have better impact strength, but also have higher shore A hardness (as shown in Fig. 2).

Analysis of coupling agent effect

The use of different kind of coupling agent produced different interaction between PVC matrix and SR/nano-CaCO$_3$ master batch and lead to different mechanical properties and ESEM morphologies of PVC/SR/nano-CaCO$_3$ nanocomposites, which further de-
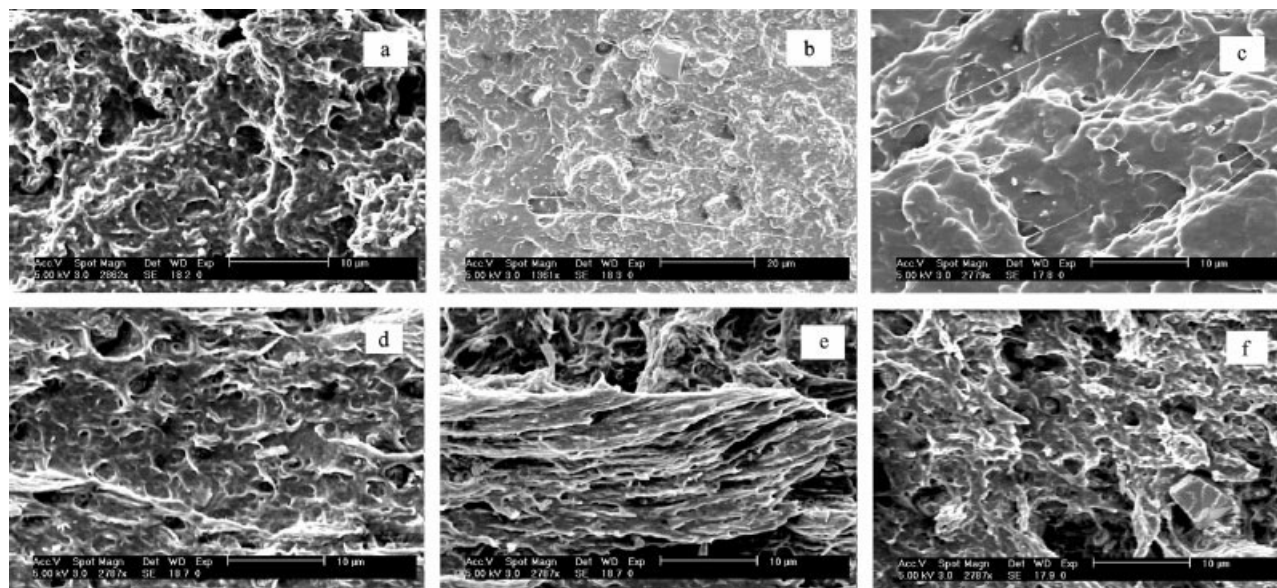

Figure 7 ESEM photographs for the fracture surfaces of (a) EPVC0; (b) EPVC1; (c) EPVC2; (d) EPVC3; (e) EPVC4; (f) EPVC5.

pends on the interfacial adhesion of the PVC matrix-SR and SR-nano-CaCO$_3$. Figure 8 compares the FTIR spectra of EPVC0–EPVC5. These nanocomposites have almost the same FTIR spectra [see Fig. 8(a)]. From Figure 8(a) it can be seen that in the spectrum of PVC nanocomposites exist aliphatic groups of CH (2960 and 2929 cm^{-1}), CH$_3$ (1380 cm^{-1}), and CH$_2$ (1450 cm^{-1}). The peaks between 3000 and 2800 cm^{-1} indicate the presence of —CH$_3$, —CH$_2$, and C—H functional groups, and the bands between 600 and 700 cm^{-1} can be attributed to C—Cl stretching vibrations. —Si—CH$_3$ absorption appeared at 1260 cm^{-1}, the —Si—O—Si— absorption had a peak at 1019, and 780 cm^{-1} was the absorption of H$_3$C—Si—CH=CH$_2$, the bands between 1620 and 1670 cm^{-1} are attributed to C=C stretching vibrations.[19,20] These results show that there are no new chemical bond between PVC matrix and SR elastomer shell and nano-CaCO$_3$ core. But the peaks marked as ''arrow'' in Figure 8(b) suggest that there are new chemical bonds formed. Analyzing every component of the PVC nanocomposites, it can be concluded that the new chemical bonds are attributed to chemical interaction of PVC and coupling agent, KH550 and KH560. The scheme for chemical interactions of PVC matrix and coupling agent are shown in Figure 10. Figure 10(a) is the intermolecular hydrogen bond between PVC and KH550; Figure 10(b–d) is the intermolecular hydrogen bonds between PVC and KH560. Obviously, (a)–(c) are stable, but (d) is unstable and instantaneous. Because of these kinds of hydrogen bonds, the interaction between PVC and SR/nano-CaCO$_3$ master batch are different as shown in Figure 11). Owing to the incorporation of intermolecular hydrogen bonds, the strong interaction between filler and polymer transformed structurally the composite into an interpenetrating polymer network [Fig. 11(d) PVC/SR/nano-CaCO$_3$ master batch ternary nanocomposite with coupling
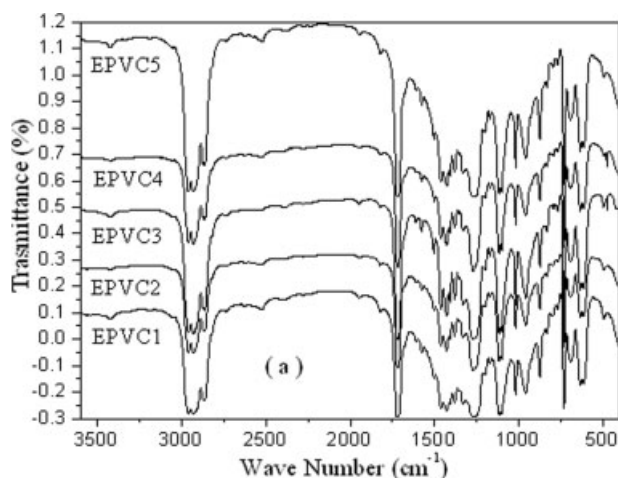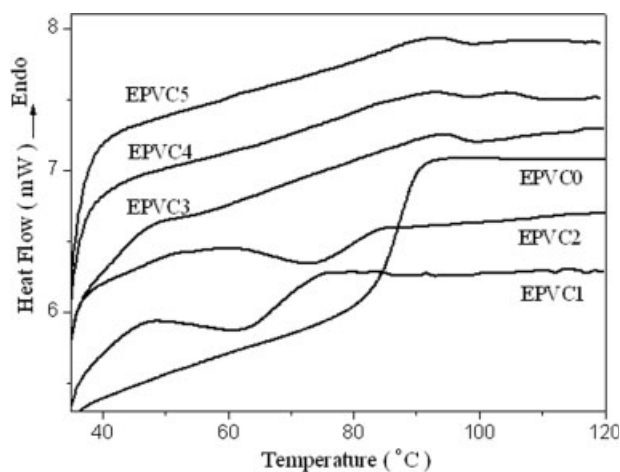

Figure 9 T_g of rigid PVC/SR/nano-CaCO$_3$ nanocomposites.

agent KH560]. So in the process of tensile, the nanocomposite EPVC4 formed oriented fasciculus in the tensile-fractured surface [Fig. 4(e)].

T_g temperatures of PVC/SR/nano-CaCO$_3$ nanocomposites also probe the interactions in these materials. Figure 9 shows the DSC curves of PVC/SR/nano-CaCO$_3$ nanocomposites. Compared with EPVC0 (T_g = 82.38°C), T_g temperatures of sample EPVC1 (T_g = 70.6°C) and EPVC2 (T_g = 79.2°C) are decreased, this result testified that SR-made nano-CaCO$_3$ particles diapered in PVC matrix well and increased the degree of molecular chain movement of PVC. Meanwhile, T_g of sample EPVC3, EPVC4, and EPVC5 are increased to 88.1°C, 99.8°C, and 88.9°C, respectively. The sample EPVC4 of SR/nano-CaCO$_3$ master batch modified with KH560 has the maximum T_g. The major driving

Figure 8 FTIR spectra for PVC/SR/nanoCaCO$_3$ nanocomposites (1) EPVC1; (2) EPVC2; (3) EPVC3; (4) EPVC4; (5) EPVC5.
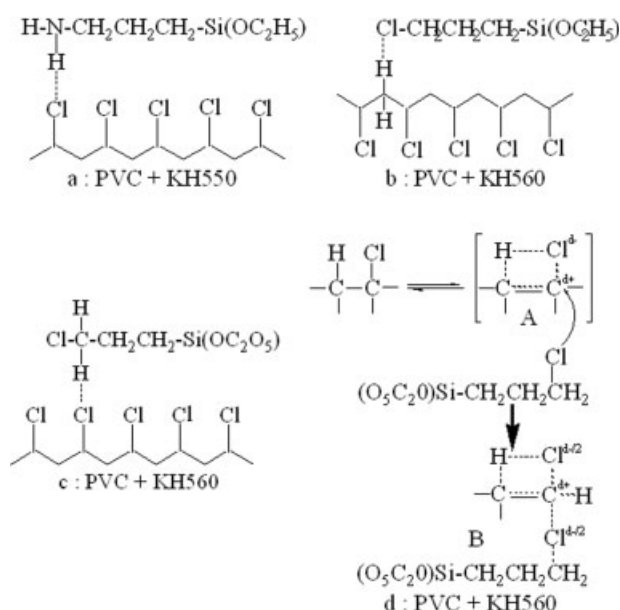

Figure 10 Schematic representation for intermolecular hydrogen bonds between PVC matrix and coupling agents (a)–(d).
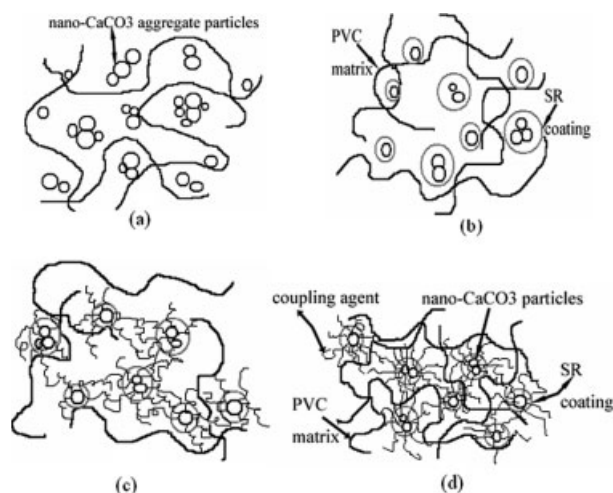
Figure 11 Schematic representation for interfacial interaction of PVC samples melt blending at 160–165°C. (a) PVC/nano-CaCO$_3$ binary nanocomposite; (b) PVC/SR/nano-CaCO$_3$ ternary nanocomposite melt blending directly; (c) PVC/(SR/nano-CaCO$_3$) master batch ternary nanocomposite with coupling agent KH550; and (d) PVC/(SR/nano-CaCO$_3$) master batch ternary nanocomposite with coupling agent KH560.

force that increases T_g of the PVC/SR/nano-CaCO$_3$ composite modified with KH560 is the interactions among PVC matrix and SR/nano-CaCO$_3$ master batch, which can prohibit the molecular chain movement of PVC.

CONCLUSIONS

Nano-CaCO$_3$/SR particle filler with core/shell structure was successfully prepared by refluxing methyl vinyl SR and nano-CaCO$_3$ particles in toluene with vigorous stirring according to an encapsulation model. And the TEM study demonstrated that the SR shell prevents nano-CaCO$_3$ particles' aggregation effectively.

The reinforcing and toughening of PVC with SR/nano-CaCO$_3$ nanoparticles were improved. A moderate toughening effect was achieved for the nanocomposites, and the elongation at break and shore A hardness also increased. The notched Izod impact strength

of nanocomposites could be improved remarkably by the incorporation of SR and coupling agent. The ESEM study indicated that the KH560-treated SR/nano-CaCO3 particles in the PVC matrix (sample EPVC4) were evenly distributed, and eliminated incompatibility between inorganic–organic interfaces effectively. The impact strength of EPVC4 containing SR/nano-CaCO3 master batch modified with KH560 is high up to 87.5KJ/m^2, tensile strength is 24.9 MPa, and elongation at break is 390.98%. Such a high toughening effect for PVC/SR/nano-CaCO3 nanocomposites was attributable to a typical rubber–plastics-toughening mechanism.

References

1. Yang, W. J.; Wu, Q. Y.; Zhou, L. L.; Wang, S. Y. J Appl Polym Sci 1997, 66, 1455.
2. Ratnam, T.; Zaman, K. Polym Degrad Stab 1999, 65, 99.
3. Yu, J.; Summers, J.; Hiltner, A.; Baer, E. J Vinyl Addit Technol 2004, 10, 11.
4. Ha, C. S.; Kim, Y. Y.; Lee, W. K.; Cho, W. J.; Kim, Y. Y. Polymer 1998, 39, 4765.
5. Matsuo, M. Polym Eng Sci 1969, 9, 206.
6. Liu, Z. H.; Zhu, X. G.; Wu, L. X.; Li, Y.; Qi, Z. N.; Choy, C. L.; Wang, F. S. Polymer 2001, 42, 737.
7. Liang, Z. M.; Wan, C. Y.; Zhang, Y.; Wei, P.; Yin, J. J Appl Polym Sci 2004, 92, 567.
8. Ren, J.; Huang, Y. X.; Liu, Y.; Tang, X. Z. Polym Test 2005, 24, 316.
9. Wan, C. Y.; Zhang, Y.; Zhang, Y. X.; Qiao, X. Y.; Teng, G. M. J Polym Sci Part B: Polym Phys 2004, 42, 286.
10. Huang, Z.; Lin, Z.; Cai, Z.; Mai, K. Plast Rubber Compos Process Appl 2004, 33, 343.
11. Zhang, Q.; Yang, H.; Fu, Q. Polymer 2004, 1913, 45.
12. Zhang, J. Z.; Wang, X.; Lu, L. D.; Li, D.; Yang, X. J. J Appl Polym Sci 2003, 87, 381.
13. He, Y. J. Powder Technol 2004, 147, 59.
14. Chen, N.; Wan, C. Y.; Zhang, Y.; Zhang, Y. X. Polym Test 2004, 23, 169.
15. Wu, D. Z.; Wang, X. D.; Song, Y. Z.; Jin, R. G. J Appl Polym Sci 2004, 92, 2714.
16. Zeng, X. F.; Chen, J. F.; Wang, G. Q. Acta Polym Sin 2002, 6, 738.
17. Renger, C. J.; Burrows, S. J.; Shanks, R. A. J Appl Polym Sci 2001, 82, 3091.
18. Giannelis, E. P. Adv Mater 1996, 8, 29.
19. Lu, J.; Ma, S. B.; Gao, J. S. Energy Fuels 2002, 16, 1251.
20. Chiu, H. T.; Chiu, S. H.; Wu, J. H. J Appl Polym Sci 2001, 89, 959.